Measurements of local radii of curvature by the retrocollimated interferometric method

J. D. Sacramento-Solano, F.S. Granados-Agustín, and A.A. Cornejo-Rodríguez
Instituto Nacional de Astrofísica Óptica y Electrónica,
Apartado Postal 51 y 216, Puebla Pue., 72000 México,
e-mail: dsolano@inaoep.mx, fermin@inaoep.mx,
acornejo@inaoep.mx

Recibido el 5 de septiembre de 2007; aceptado el 14 de mayo de 2008

With the measurements of the local radii of curvature of an aspherical optical, convex or concave surface, the shape of the surface can be found. In this paper a method is proposed for taking radius measurements, for off-axis sections of an optical surface, using a retrocollimated interference method (rim) that was previously developed by several authors[1-3]; but in particular, in this paper, the one described by Xiang[4] for measuring long radii of curvature[5,6] is used.

Keywords: Retrocollimated; interference; radii of curvature.

A partir de las medidas de los radios de curvatura locales, de una superficie asférica convexa ó cóncava, se puede encontrar la forma de dicha superficie. En este trabajo se propone un nuevo método para medir los radios de curvatura locales, de una superficie fuera de eje, usando un método interferométrico por retrocolimación, desarrollado anteriormente por varios autores para superficies en eje[1-3]; en particular en este trabajo se usa el método desarrollado por Xiang[4], cuya característica principal es medir radios de curvatura largos[5,6].

Descriptores: Retrocolimación; interferencia; radios de curvatura locales.

PACS: 42.87.-d; 42.79.Bh; 42.25.Hz

1. Introduction

There are many methods for measuring the paraxial radius of curvature of optical surfaces[7 - 9], and the techniques employed could be mechanical (for example in the Computerized Numerical Control (CNC) machine tool, stylus instruments, etc.) [10,11] or optical (with Fizeau interferometers in the visible and infrared wavelengths) [12]. The methods using interferometric techniques are, in general, more accurate for setting certain positions, such as the center of curvature (c.c.), and the vertex (v) of an optical surface[13]. There are several papers that reported using an interferometer, where the outgoing and returning light beams from the interferometer are collimated and retrocollimated, respectively. In all the experimental arrangements using this retrocollimated technique, as is common in some other methods, the main aim is to find the c.c. and vertex of the surface; that means that for long radii of curvature measurements, some of the optical components or the optical surface have to be moved long distances (Non-Contact Measurements) [14]. In order to solve the problem for long distance shifting of the optical parts of the instrument, or the optical surface, for long radius of curvature measurements, there are some techniques using auxiliary optics, such as those developed by Mingshan[3] and Xiang[4]. In particular, the work by Xiang used a simple but powerful method based on Newton's equation for lenses[5,6].

2. Retrocollimated interferometric method

In what follows, as a brief explanation, the main steps to be applied in the method described by Xiang are described [4]; in this paper the XIang method is applied to measure the local radii of curvature of a monolithic conic surface and off-axis conic section.

Figure 1a shows the collimated beam passing the beam splitter (BS_1) and moving toward the lens L; the beam is focused on the back focal point, F_1', of lens L_1 that is located on the vertex V of the surface, S.

For the use of the retrocollimated beam for finding the front focal point F_1 of L_1, at O, see Fig. 1b; a second auxiliary lens, L_2, and a flat mirror, M, are positioned as shown in Fig. 1b. Once the point $F_2' = F_1$ is located, the flat mirror is removed from the experimental setup.

In Fig. 1c, the lens L_2 is shifted to the left a distance x, for a convex surface, because the idea is to locate O" = *cc* for the vertex or off-axis zone, because at this position, a retrocollimated beam is produced and returned to the left. This means that when the c.c. is coincident with O", and taking the fact that the vertex was previously was coincident with the focal point F_1', then the value of the radius of curvature of the surface can be obtained from Newton's equation[15,16]

$$xx' = -f^2; \tag{1}$$

since $f = f_1$ and x is measured and $x' = R$, therefore,

$$R = -f_1^2/x \quad . \tag{2}$$

For the case of a concave surface, the lens L_2 is shifted to the right, because the *cc* is in front of the surface.

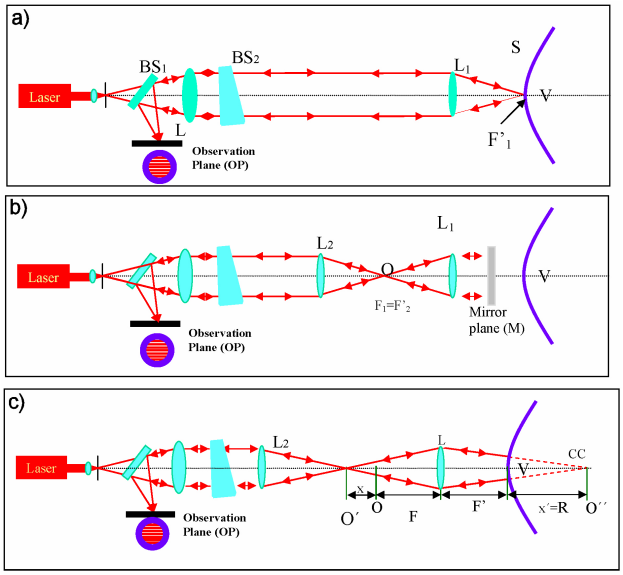

FIGURE 1. a) Observed interference fringes at OP by retrocollimated beam from vertex V. b) Retrocollimated beam reflected on flat mirror M, once confocal arrangement is set up with lenses L_1 and L_2. c) Similar to a) and b), a retrocollimated beam from the surface is obtained when O" is the image O'.

From the above explanation, it can be seen, by the Gaussian relation between image and object distances, that with a short shifting of lens L_2, corresponding to the distance x, a long paraxial radius of curvature of an optical surface can be measured. As a matter of fact the radius of curvature could be in the order of meters. Appendix A explains a general method for the selection of the set of lenses L_1 and L_2 for contructing an experimental setup with different dimensions. A specific example of the selection of the lenses of the experimental scheme is given for the case of a conic convex surface[12], with local radii of curvature between 176.50, at the vertex, and 363.79 cm, at the edge.

It is important to mention that in the paper by Xiang [4] there is an extensive error analysis of the retrocollimated interferometric method, using the Newton's equation for a lens. As a complement to such error analysis, in Appendix B there is a further study of the errors, but for the case of shorter radius of curvature measurements,$i.e.$ less than one meter.

3. Measurement of local radii of curvature of an aspherical or conic optical surface

As has been mentioned previously, in what follows it is explained how the (rim) method[16] for measuring paraxial radius of curvature[4] can be extended and applied to measurements of the local radii of curvature of a monolithic conic surface, and also for an off-axis section of a parabolic surface. This is done because, as an alternative method, from the knowledge of the local radii of curvatures, the shape of a surface can be found.

3.1. Monolithic conic surface

For the measurements of local radii of curvature (LRC) for an off-axis zone, Fig. 2a shows the experimental scheme used in our experiment. Figure 2b shows a diagram indicating how the surface must be first shifted by a distance Y, using the vertex of the surface as a reference starting point, for fixing certain off-axis zones of the optical surface; as a second step the surface is rotated through an angle θ around a vertical axis fixed at the "vertex"; and the third step is to define the "vertex" of the off-axis section. In the lower picture in Fig. 2a, the mechanical mounts used to rotate and shift the surface under test can be seen. In order to take the measurement of the LRC, the steps in Fig. 1b and 1c must be completed. For decreasing the focusing contribution to the error in the method, mentioned in the Appendix B, for the different zones of the surface, a diaphragm is used when the surface is illuminated[5].

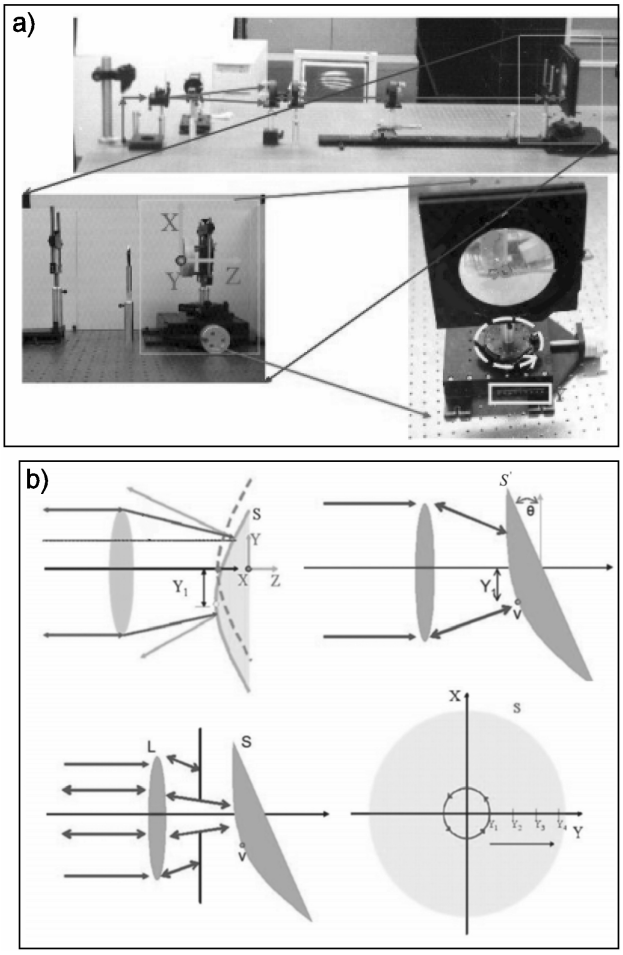

FIGURE 2. a) Upper picture a general view of the experimental setup. Lower left picture is a lateral view of the mounting of the surface, with L_1axis along the optical axis. Lower right, front view of the surface, showing rotation of the surface under measurement around a vertical axis. b) Schematic view of the translation, Y_1 and rotation θ of the surface around the vertical axis; to find out the zones, Y_1, along which the radii of curvature are measured.

The requirements for rotating and shifting the surface certain angle and distance, as shown in Fig. 2b, are in order to ensure that the incident beams are normal to the surface, so that a reflected and retrocollimated beam comes back from the surface; of course, as shown in the experimental scheme in Fig. 1c, for finding the value of LRC, the lens L_2 must be shifted.

For the case of a parabolic surface, with conic constant $K = -1$, a diameter of 150 mm, and paraxial radius of curvature (prc) $r = 596.6$ mm. The interferograms observed along different diameters and local positions are shown in Fig. 3; as a numerical example, the values of Table I are for the local positions, along the Y axis, with $x = 0$. For the different values of Y, a comparison is made between the theoretical and experimental values of the local radii of curvature. The rotated angle θ is fixed for each position and measurement are done, until an interferogram is observed in the observation plane (op). The interferograms of Fig. 3 are taken after the accomplishment of normal incidence beam to each off-axis zone of the surface, and after following the procedure of Fig. 1c and the explanation given in Sec. 2 for this step.

TABLE I. Parabolic surface with a diameter of 150 *mm.* and prc equal to 596.6 mm.

Y(mm)	R_{teo}(mm)	R_{Exp}mm)
0	596.610 ±0.001	596.562±0.017
21.05	597.284	597.449 ±0.017
29.55	598.073	598.071 ±0.017
38.05	599.035	599.301 ±0.017
46.55	600.239	600.598 ±0.017

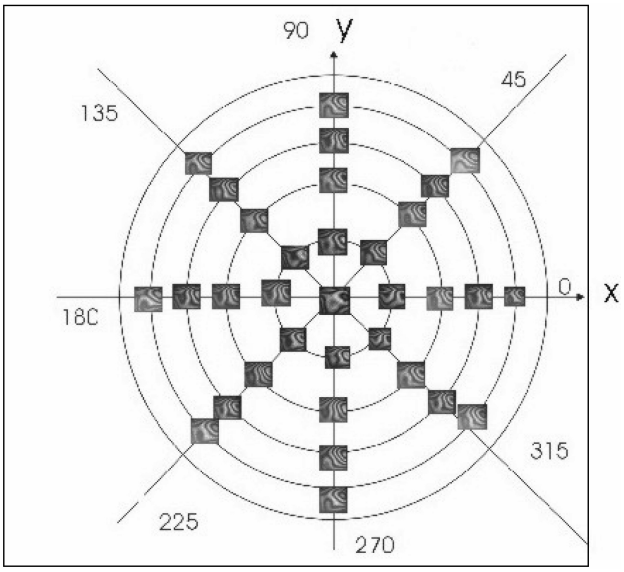

FIGURE 3. Interference patterns observed at the locations where radii of curvature measurements are done, for a monolithic surface.

It is worth mentioning that the accuracy of the measurements can be achieved because the positions of the retrocollimated beams produced the interferograms of Fig. 3 and the interferogram has a minimum number of fringes. Hence, for 10 measurements for each position, the same interference pattern must be observed; and for each zone the interferogram has the minimum number of fringes.

3.2. Off-axis section of a conic surface

For this case, it is necessary to satisfy the same condition that the incident beams upon the optical surface must be normal to the surface; Fig. 2b already shows the rotated angle and shift motions required for the off-axis zones of a monolithic surface. However, for an off-axis section, because the definition of the optical axis and vertex of the surface are unknown throughout the experiment, an additional shift is compulsory along the Z direction. The correct new shift along the Z direction, after rotation through an angle θ and motion along the y direction, can be found by looking, once more, at the observed interferograms and finding the ones with the least number of fringes[6]. As in the case of a monolithic surface, for each position ten measurements are taken.

As in the previous case, Sec. 3.1, Fig. 4 shows the interferograms observed along one diameter, and Table II shows the theoretical and experimental results for a parabolic off-axis section. The off-axis section is 130 mm. from the optical axis, and the paraxial radius of curvature (prc) is 2415 mm.

Finally we can obtain the shape of the surface using the values of the LRC, and its values are adjusted by a numerical method[20]. Another method for finding the surface shape was with the use of a genetic algorithm[21]; this generated a population of surfaces, until the best surface fitting the local radius of curvature values was found.

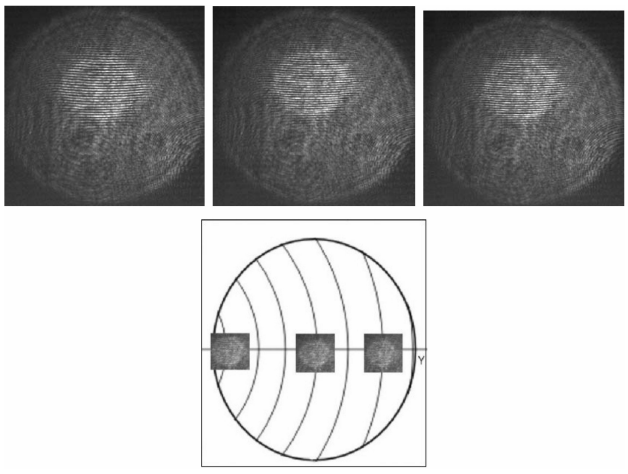

FIGURE 4. Interference patterns observed at three locations, for the measurements of the radius of curvature for an off-axis section of a parabolic surface.

TABLE II. Measurements for an off axis, 130 mm from the optical axis, and prc equal to 241.5 mm.

Y (mm)	*Rteo* (mm)	*Rexp* (mm)
50	2416.553	2417.357
107	2422.334	2422.187
130	2425.504	2425.565

4. Conclusions

An extended method has been developed for the measurements of local radii of curvatures either at the vertex, on-axis and off-axis sections of a monolithic surface; or for an off-axis conic surface. The method is very suitable for long radius of curvature measurements, mainly for optical surfaces with a large range of values for radii of curvature (see Appendix A). The results shows some difference between the theoretical and experimental results, and are given in Tables I and II; it can be seen that such differences are within acceptable errors. The method is consistent for taking several measurements for the same position on the surface, because the technique used by observing interferograms for fixing the positions for the center of curvature and vertex enable us to have greater accuracy. From this knowledge of the local radii of curvature, the profile of the surface along different diameters can be found; therefore, the shape of the surface can also be known. For the case of fast optical surfaces, the described method could also be useful.

After the application of Xiang's method for off-axis sections, explained in this paper, in Appendix A and B, further studies were done into this technique. Appendix A explains how the test system can be designed for the lenses L_1 and L_2, and in Appendix B an error analysis is given for the case of short radii of curvature, less than 1000 mm.

Acknowledgments

This research was supported by CONACyT-México under projects P49699-F and 50395-F. We also wish to thank Miss Ana María Zarate-Rivera and the technicians of the INAOE Optical Shop, as well as the referee for his valuable comments.

Appendix

A. Selection of focal length of lenses L_1 andL_2, and the overall-length of the experimental arrangement of lenses L_1 andL_2.

One aspect to consider for the experimental setup, is that the distance between the lens in front of the surface under test could be selected and depends on the characteristics of the experimental setup, but assuming that the lenses in the optical setup shown in Fig. 1 and Fig. 5 have the same focal length $f_1 = f_2 = f$. Figure 5 shows that once the vertex, V, of the surface is fixed, the lens L_2 must be shifted a distance x, in order to find the center of curvature O'' such that O'' is the image of O'. Hence the maximum distance,D, of the set of lenses, where one of them is shifted a distance$x$, is equal to

$$D = 3f + x. \tag{A.1}$$

Using the thin lens equation

$$\frac{1}{f} = \frac{1}{l'} - \frac{1}{l}, \tag{A.2}$$

from the same Fig.5, the next equation for lenses can be written

$$\frac{1}{l} = \frac{1}{l'} - \frac{1}{f} = \frac{1}{r+f} - \frac{1}{f} = \frac{f-r-f}{f\,(r+f)} = \frac{r}{f\,(r+f)};$$

and therefore

$$x = l - f,\ l = \frac{f\,(r+f)}{r}\ ;\ x = l - f. \tag{A.3}$$

In order to find the changes in the distances$x$, for the shifting of lens L_2, and the overall distance, D, for different values of the focal distance,f, of the lenses, the following particular case is analyzed.

For the convex secondary mirror of the Large Millimeter Telescope (LTM)[17], the following characteristics are considered for its convex surface: paraxial radii of curvature r = 176.5cm, diameter ϕ = 250cm, and conic constant k = - 1.14269, which correspond to a hyperbolic surface. In Table III, it is shown that once the focal distance is chosen($f = f_1 = f_2$), and using Eqs. (A.1) and (A.3), the values of $l,\ x,$ and D can be calculated. From the same Table III, for shorter values of f, a more compact lens system are implied, and smaller shifts for x are required; in other words, D and x have smaller values.

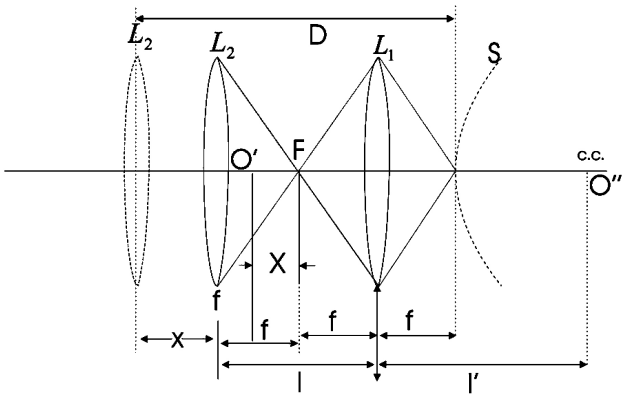

FIGURE 5. Diagram for the lens L_1 and L_2 in a confocal setup; shifting lens L_2 by amount x, such that O" = c.c., and O" is the image of O'. D is the overlength of the experimental set up of lenses L_1 and L_2.

TABLE III. Relations between parameters of the setup of Fig. 5, and using Eqs. (A.1) to (A.3).

f	l'	x	$\sim D$
1000	15665	565	3565
500	641.6	141.6	1641.6
400	490.6	90.6	1290.6
300	351.0	51.0	951.0
250	285.4	35.4	785.4
200	222.7	22.7	622.7

Units are in mm.

TABLE IV. Example of Δr_z vs x, with f = 30 mm, and hyperbolic surface with k = - 1.14269, and diameter of 2500mm.

S(mm)	r_z(mm)	x(mm)
250	1829.5	49.2
500	2016.4	45.0
750	2346.9	38.8
1000	2821.5	32.3
1250	3482.4	25.8

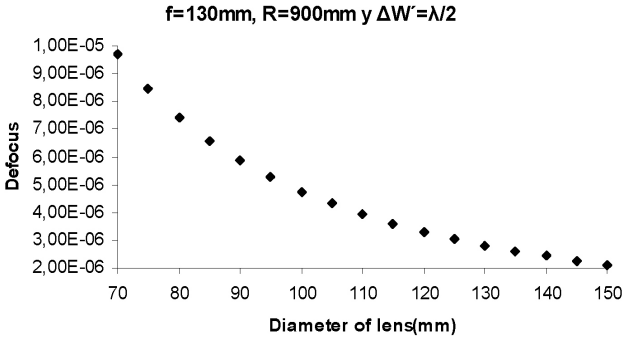

FIGURE 6. Decreasing of focusing error with the bigger diameter of lens, in the setup of Fig. 1a. with f=130 mm.

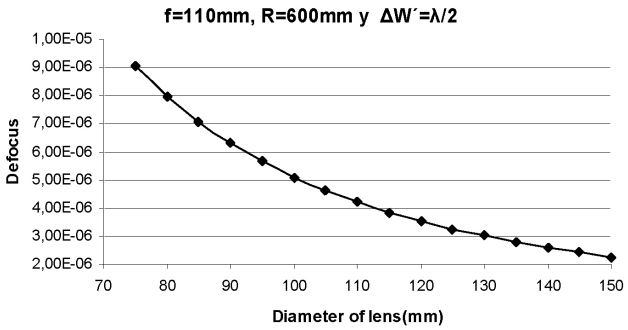

FIGURE 7. Decreasing of focusing error with the bigger diameter of lens, in the setup of Fig. 1a. with f=110 mm.

Using the equation $r_z = (1/c)\left(1 - kc^2S^2\right)$[18], where c is the paraxial curvature of the surface, Table IV shows, for the same surface described above, the corresponding local radii of curvature (r_z) for different zones, S, of the surface. Considering that the focal distance of lenses L_1 and L_2 of the experimental setup are both equal to 30 cm; with Eq. (A.3) the corresponding data for the shifting distance x is calculated. From the same Table IV, it can be concluded that, for an interval Δr_z = 165.29cm, the interval for moving lens L_2 is only Δx = 2.34cm. With this example, it is important to notice the capacity of the method, and the necessity to find out the most adequate values for the focal distances of L_1 and L_2 of Fig. 5.

B. Error analysis for short radii of curvature

In this section we derived the error analysis of this method; from Eq.(2) is derived the equation

$$\delta R = \left|\frac{\partial R}{\partial f}\right| \Delta f + \left|\frac{\partial R}{\partial x}\right| \Delta x; \tag{B.1}$$

where implicit form is

$$\delta R = \frac{2f}{x}\Delta f + \frac{f^2}{x^2}\Delta x; \tag{B.2}$$

and the relative error with respect to R is

$$\frac{\delta R}{R} = \left(\frac{\frac{2f}{x}}{\frac{f^2}{x}}\right)\Delta f + \left(\frac{\frac{f^2}{x^2}}{\frac{f^2}{x}}\right)\Delta x = \frac{2\Delta f}{f} + \frac{\Delta x}{x}. \tag{B.3}$$

But we need to consider the contribution of the focusing error, which can be analyzed as follows:

$$\frac{\delta R}{R} = 2\frac{\Delta f}{f} - \frac{\Delta x}{x} + \frac{\Delta t}{R}; \tag{B.4}$$

where Δf, Δx, and Δt, are errors in the focal length, with the distance, , and the focus position , respectively. The condition imposed for dropping the error Δt is that $|\Delta t/R| < 10^{-6}$, which is satisfied for the experimental setup. Then, from the error analysis, and taking only the first two terms of Eq. (B.4), an accuracy of 0.1% can be obtained for surfaces with R > 100cm.

For the case of surfaces with R < 100cm, the following error analysis is done in order to eliminate the influence of the third right term of Eq. (B.4), considering the equation derived by Hopkins[18], for the defocus term, to be

$$\frac{\Delta t}{R} = \left[8\left(\frac{f}{\phi}\right)^2 \Delta w\right] \Big/ R; \tag{B.5}$$

Figures 6 and 7, shows the change in defocus, according to Eq. (B.2), as a function of the diameter ϕ of the lens, with $\Delta w = \lambda/2$; for R = 900mm and f = 130mm; and R = 600mm and f = 110mm, respectively. It can be seen from the first case, Fig. 6, that the diameter required must be larger than 95mm; from Fig. 7 the diameter must also be larger 95mm. Hence in order to satisfy the condition for eliminating the influence of defocus, Δt, from Eq. (B.4), for R <10cm, a set of adequate values of f and ϕ must be chosen.

1. M.C. Gerchman and G.C. Hunter, *Opt. Eng.* **19** (1980) 843.
2. M.V.R.K. Murty and R.P. Shukla, *Opt. Eng.* **22** (1983) 231.
3. Mingshan Zhao, Jing Yaling, and Li Guohua, *Proc. SPIE* **2536** (1995) 498.
4. Xiang Yang, *Appl. Opt.* **40** (2001) 6210.
5. F.S. Granados-Agustín, J.F.M Escobar-Romero, J.D. Sacramento-Solano, and A. Cornejo-Rodríguez, *Proc. SPIE* **5252** (2003) 272.
6. J.D. Sacramento Solano, F. Granados Agustín, and A. Cornejo Rodríguez, *Proc. SPIE* **5622** (2004) 663.
7. R.H. Noble, *Optical shop Testing*, ed. D. Malacara (John Wiley & Sons, New York, 1978) Chap. 15, p.459.
8. J.H. Bruning, *Optical shop Testing*, ed. D. Malacara (John Wiley & Sons, New York, 1978) Chap. 13, p. 428.
9. L.A. Selberg, *Opt. Eng*. **31** (1992) 1961.
10. Wayne Langdon, *Proc. SPIE* **1168** (1989) 51.
11. M. Stedman and K. Lindsey, *Proc. SPIE* **1009** (1989) 56.
12. M. Ferrari, S. Mazzanati, and G. Lemaître, *Proc. SPIE* **2576** (1995) 270.
13. R. Geyl and J. Paseri, *SPIE* **2775** (1996) 476.
14. D.C. O'Shea and S.A. Tilstra, *SPIE* **0966** (1988) 172.
15. Hardy A. and F. Perrin, *Principles of Optics* (Mac Graw Hill Co., New York, 1932) p. 371.
16. F.A. Jenkins and H.E. White, *Fundamentals of Optics*, fourth ed., (Mc Graw Hill - Kogakusha, Ltd, Tokyo, 1965) p. 73.
17. Instituto Nacional de Astrofísica, Óptica y Electrónica, *The Large Millimetric Telescope Homepage*, http://binizaa.inaoep.mx/; mail address, Apdo. Postal 51 y 216, 72000 Puebla, Pue. México.
18. H.H. Hopkins, *Wave Theory of Aberrations* (Oxford University, London, 1950) p. 141.
19. J. Ojeda Castañeda, *Optical shop Testing*, ed. D. Malacara (John Wiley & Sons, New York, 1978) Chap. 8, p.298.
20. A. Magaña and J.H. Pascual, MC Thesis, National Institute of Astrophysics Optics and Electronics, Puebla, México, 1996.
21. A. Santiago-Alvarado, S. Vázquez-Montiel, R. Nivón-Santiago, and C. Castañeda-Roldan, *Rev. Mex. Fís.* **50** (2004) 358.